New Zealand Journal of Geology and Geophysics
Vol. 55, No. 3, September 2012, 305–311

Statistical analysis of the 2010 M_W 7.1 Darfield Earthquake aftershock sequence

R Shcherbakov[a,b]*, M Nguyen[a] and M Quigley[c]

[a]*Department of Earth Sciences, University of Western Ontario, Ontario, Canada;* [b]*Department of Physics and Astronomy, University of Western Ontario, Ontario, Canada;* [c]*Department of Geological Sciences, University of Canterbury, Christchurch, New Zealand*

(*Received 14 December 2011; final version received 8 March 2012*)

Statistical properties of the aftershock sequence of the M_W 7.1 Darfield (Canterbury, New Zealand) earthquake are studied. The sequence exhibits rich scaling behaviour in magnitude and aftershock decay rates. In particular, we observe a marked variability in the frequency-magnitude statistics in space, between early and late times after the mainshock and over different magnitude ranges. The mainshock triggered two large earthquakes (22 February 2011 M_W 6.2 Christchurch earthquake and 13 June 2011 M_W 6.0 earthquake) that occurred later in the sequence and generated their own aftershock sequences. The frequency-magnitude statistics of the sequences are modelled using the Gutenberg–Richter scaling relation. We also study the difference between the magnitudes of the largest recorded aftershocks and the mainshock. This is analysed and discussed using the modified Båth law. In this context we consider the M_W 6.2 Christchurch and 13 June 2011 M_W 6.0 earthquakes as the largest aftershocks of the Darfield mainshock. It is also observed that the aftershock decay rates can be approximated by the modified Omori law. The obtained results indicate that the aftershock sequence exhibits self-similarity in both magnitude and time.

Keywords: aftershocks; Båth law; Darfield mainshock; Gutenberg-Richter scaling; modified Omori law

Introduction

The M_W 7.1 (m_L 7.1) Darfield (Canterbury, New Zealand) earthquake, which occurred on 4 September 2010 (all reported dates are NZ standard time), was the largest surface-rupturing continental earthquake in New Zealand since the 1968 M_W 7.1 Inangahua earthquake. The dominant moment release in the Darfield earthquake resulted from the rupture of the previously unrecognised Greendale Fault (Quigley et al. 2010), although the rupture sequence involved a complex array of at least three other faults (Fig. 1; Beavan et al. 2010). This earthquake involved a relatively high ‘stress drop’ of 14–16 MPa (Fry et al. 2011; Quigley et al. 2012) and generated a rich aftershock sequence (termed the Canterbury earthquake sequence) including the 22 February 2011 M_W 6.2 (m_L 6.3) and 13 June 2011 M_W 6.0 (m_L 6.4) Christchurch earthquakes (source: GNS Science GeoNet: http://magma.geonet.org.nz/resources/quakesearch/). Geodetic and InSAR data imply that both of these large aftershocks similarly involved more than one fault rupture on previously unrecognised faults to the south and southeast of the Christchurch central business district (CBD; Beavan et al. 2012). The proximity of these aftershocks to the city, rupture directivity and other characteristics of the ruptures resulted in significantly higher recorded ground accelerations and amounts of damage relative to the September mainshock (Fry et al. 2011) and, in the case of the February event, numerous fatalities. These two earthquakes can be considered as triggered aftershocks of the original Darfield earthquake because they occurred in the region surrounding the Darfield earthquake epicentre that experienced early aftershocks. Each of these two earthquakes also generated their own aftershock sequences. These events highlight the importance of studying aftershock statistics to better understand seismic hazard during an earthquake sequence.

This paper examines the statistical properties of the aftershock sequence triggered by the 2010 Darfield mainshock. We presented a comprehensive analysis of the frequency-magnitude statistics of the sequence by studying its temporal and spatial evolution. We also analysed the statistics of the aftershocks of two large earthquakes which occurred later in the sequence. In addition, we analysed temporal decay rates of aftershocks of each sequence and model them using the generalised Omori law approach (Shcherbakov et al. 2004). We computed the difference between the magnitude of the largest observed aftershock and the magnitude of the mainshock. This difference reflects another empirical law known in seismology as Båth’s law (Båth 1965). By using the modified form of Båth’s law (Shcherbakov & Turcotte 2004) it has been possible to estimate the inferred largest aftershock from the extrapolation of Gutenberg–Richter scaling.

The Darfield earthquake provides a good opportunity to study in detail the temporal scaling properties of aftershock sequences generated by large ($M_W > 7.0$) strike-slip mainshocks. In New Zealand, the majority of large strike-slip

*Corresponding author. Email: rshcherb@uwo.ca

ISSN 0028-8306 print/ISSN 1175-8791 online

http://dx.doi.org/10.1080/00288306.2012.676556
http://www.tandfonline.com

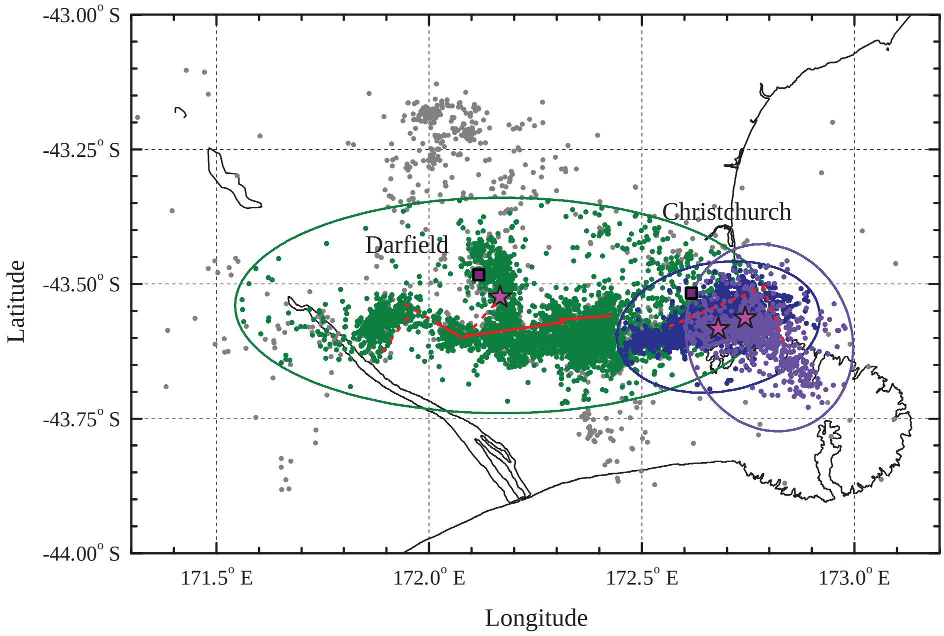

Figure 1 Subdivision of the aftershock region into three regions, based on the occurrence of aftershocks in the Darfield sequence. The first elliptical zone contains the aftershocks that occurred after the Darfield mainshock for 171 days. The second elliptical zone delineates the aftershock cluster of the Christchurch mainshock for 112 days. The third zone contains the aftershocks that occurred after the 13 June 2011 mainshock. The earthquakes above magnitude 2.5 are shown. Projected surface location of blind faults with $M_W \geq 6.0$ (dashed line) from http://www.geonet.org.nz/canterbury-quakes/ and location of Greendale Fault surface rupture (solid line) from Quigley et al. (2012).

earthquakes have occurred in sparsely populated regions. This is clearly not always the case and, in this instance, no fatalities were recorded in the mainshock while 281 fatalities were recorded from the 22 February aftershock. Aftershocks are an essential part of any major seismic sequence. They occur due to static and dynamic stress redistribution in the vicinity of major earthquakes (Kisslinger 1996; Shcherbakov et al. 2005). They also represent an outcome of complex triggering mechanisms which operate in a highly heterogeneous system of non-linearly interacting faults embedded in a visco-elastic medium (Ben-Zion 2008). A deeper understanding of the mechanisms and physics of aftershocks is therefore of crucial importance. The present study aims to provide detailed and accurate statistical inferences about the Darfield aftershock sequence within the limitations set by the data. Such detailed studies will lead to a better understanding of the aftershock process in general.

Statistical analysis

Data selection

In this study, we used the GeoNet earthquake catalogue for our analyses where the magnitude reported was m_L (http://magma.geonet.org.nz/resources/quakesearch/; the catalogue was downloaded on 23 December 2011). The earthquakes above magnitude 2.5 are shown in Fig. 1 for 564 days after the Darfield mainshock. The major problem encountered in the studies of aftershocks is the lack of reliable data, especially immediately after a mainshock. Detailed analysis of aftershock sequence waveforms reveals that a significant number of early events are missing in existing catalogues (Peng et al. 2006, 2007). This is generally ascribed to the dramatic increase in the number of events in the wake of a large mainshock and its large aftershocks. This masking of smaller magnitude aftershocks further complicates the omnipresent problem of defining a minimum magnitude of completeness for the catalogue.

The catalogue used here was complete only for events greater than $m_L \geq 3.0$. This value was estimated from the histogram plots of the frequency-magnitude distributions given in Fig. 2. For most fitting purposes we used a completeness magnitude m_c of 3.0. A contentious issue for the analysis of any aftershock sequence is the choice of the spatial domain for the study. In this study, the aftershock regions (shown in Fig. 1) were chosen based on the early distribution of aftershocks and the rupture dimension of the M_W 7.1 (m_L 7.1) Darfield mainshock (4 September 2010) and its two largest aftershocks (M_W 6.2 (m_L 6.3) 22 February 2011 event and M_W 6.0 (m_L 6.4) 13 June 2011 event). We defined three elliptical regions surrounding the original Darfield mainshock as well as the other two triggered events to delineate the corresponding aftershock zones. To define the spatial extent of each aftershock sequence, we used the early aftershock patterns after each event to outline the extent of each aftershock zone (Fig. 1).

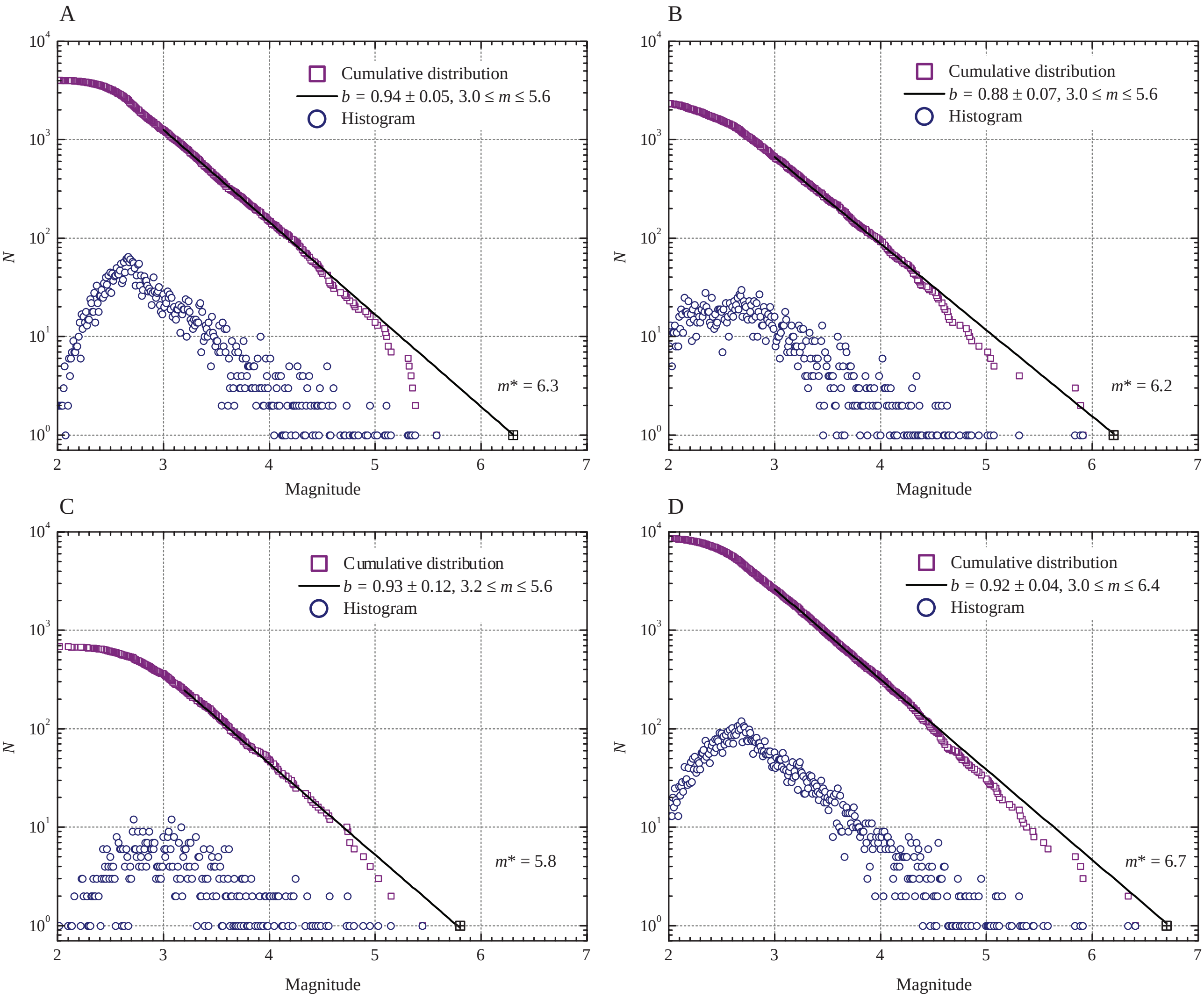

Figure 2 Cumulative $N(\geq m)$ frequency-magnitude distribution (open squares) for the various aftershocks. **A,** Darfield mainshock (3 September 2010) for 171 days. **B,** Christchurch 6.2 M_W mainshock from 22 February 2011 until 13 June 2011. **C,** 13 June 2011 M_W 6.0 mainshock for 180 days after the event. **D,** Entire aftershock sequence of the M_W 7.1 Darfield mainshock for 564 days after the mainshock. The solid line represents the GR scaling relation with the parameters computed using the maximum likelihood method. The magnitudes of the inferred largest aftershocks m^* are also given. The incremental $N(=m)$ frequency-magnitude distribution (open circles) is also shown.

Frequency-magnitude statistics

The frequency-magnitude statistics of earthquakes can be described by the Gutenberg–Richter (GR) scaling relation (Gutenberg & Richter 1954). This scaling is defined as

$$\log_{10} N(\geq m) = a - bm, \qquad (1)$$

where $N(\geq m)$ is the number of earthquakes with magnitudes greater that or equal to magnitude m and a and b are constants. This relationship holds for global earthquake catalogues and is also applicable to aftershock sequences. The estimation of the b-value has been subject of considerable research and various methods exist (Bender 1983; Tinti & Mulargia 1987; Guttorp & Hopkins 1986; Bhattacharya et al. 2011).

The cumulative frequency-magnitude distribution of the aftershocks of the M_W 7.1 (m_L 7.1) Darfield mainshock is shown in Fig. 2A. This distribution was constructed over 171 days before the occurrence of the M_W 6.2 Christchurch earthquake on 22 February 2011. This earthquake can be considered as an aftershock of the original Darfield mainshock, which generated its own sequence of aftershocks (Fig. 1). In Fig. 2B we plot the corresponding frequency-magnitude distribution of that secondary aftershock sequence. The time interval of 112 days was used to construct this distribution. The end of this time interval was marked by the occurrence of a large earthquake with magnitude M_W 6.0 which struck on 13 June 2011. This earthquake triggered the third aftershock cluster (Fig. 1). The frequency-magnitude

Table 1 The *b*-values and *a*-values of the GR scaling relation and the parameter of the modified Omori law *p* for the three aftershock sequences considered. *N* is the number of aftershocks for each sequence considered greater than or equal to $m \geq 3.0$ except for the last sequence where $m \geq 3.2$. The parameters were estimated using the maximum likelihood method and all the errors are reported at 95% confidence level.

Sequence	*b*	*a*	*p*	*N*
Darfield mainshock	0.94 ± 0.05	5.91 ± 0.16	1.21 ± 0.11	1254
Christchurch event	0.88 ± 0.07	5.46 ± 0.20	0.85 ± 0.04	664
13 June event	0.93 ± 0.12	5.36 ± 0.37	0.88 ± 0.05	360

distribution of this aftershock sequence is given in Fig. 2C for 180 days after the 13 June earthquake.

The frequency-magnitude statistics of these three aftershock sequences were modelled using the GR scaling relation. The parameters were estimated using the maximum likelihood method (Bhattacharya et al. 2011). For the main Darfield aftershock sequence, we obtained $b = 0.94 \pm 0.05$ and $a = 5.91 \pm 0.16$. For the Christchurch sequences the computed values were $b = 0.88 \pm 0.07$ and $a = 5.46 \pm 0.20$. Finally, for the sequence generated by the 13 June mainshock, the GR parameters were $b = 0.93 \pm 0.12$ and $a = 5.36 \pm 0.37$. The obtained *b*-values are within error limits of each other (Table 1). Higher magnitude cut-offs essentially give the same values (not reported here).

Assuming that the Darfield mainshock and the other two $M_W > 6.0$ events formed one complex aftershock sequence, we examined its frequency-magnitude statistics and the corresponding GR scaling (Fig. 2D). The spatial area for this combined sequence was chosen as a square box of size $0.8^o \times 1.8^o$ centred on the epicentre of the Darfield mainshock. The maximum likelihood estimated values of the parameters of the GR relation were $b = 0.92 \pm 0.04$ and $a = 6.17 \pm 0.11$.

The largest aftershock and Båth's law

Within the aftershock sequence generated by a large mainshock, the largest aftershock possesses significant additional hazard. The difference in magnitude between the mainshock and its largest aftershock has been the topic of several studies (Båth 1965; Vere-Jones 1969; Console et al. 2003; Helmstetter & Sornette 2003; Shcherbakov & Turcotte 2004). This difference constitutes the so-called Båth's law and is defined as $\Delta\bar{m} = m_{\text{ms}} - m_{\text{as}}^{\max}$, where m_{ms} is the magnitude of the mainshock and $m_{\text{as}}^{\max}$ is the magnitude of the largest recorded aftershock (Båth 1965). The averaging is done over many aftershock sequences. In general, $\Delta\bar{m}$ is considered to be a constant, $\Delta\bar{m} \approx 1.2$, independent of the mainshock magnitude (Båth 1965).

The Darfield aftershock sequence triggered several large aftershocks. The first large recorded aftershock in the sequence (m_L 5.6) occurred within 21 minutes of the mainshock. The largest aftershock in terms of m_L occurred on 13 June 2011 and had a m_L of 6.4 and M_W of 6.0. The second-largest aftershock can be considered the m_L 6.3 (M_W 6.2) 22 February 2011 Christchurch earthquake. Using the magnitude of the largest recorded aftershock (13 June 2011 event), the difference in local magnitude yields $\Delta m = 0.7$, which is lower than expected from Båth's law. It should be noted however that Båth's law is a statistical statement ($\Delta\bar{m} \approx 1.2$ only when averaged over many aftershock sequences) and does not strictly apply to individual aftershock sequences.

Here we try to infer the largest aftershock magnitude from the GR law and fit it into the standard picture of Båth's law following Shcherbakov & Turcotte (2004). We set $N = (\geq \text{m}) = 1$ in the GR scaling law to obtain $a = bm^*$, where m^* represents the largest inferred aftershock. By combining the latter statement and Equation (1), we obtain

$$\log_{10} N(\geq m) = b(m^* - m). \tag{2}$$

The analysis of ten aftershock sequences in California revealed that $\Delta m^* = m_{\text{ms}} - m^* \approx 1.11$ with the standard deviation of 0.29 (Shcherbakov & Turcotte 2004). This will be referred to as the modified Båth law.

Using this latter approach, it was possible to calculate the difference in magnitude between the Darfield mainshock (m_L 7.1) and the largest inferred aftershock. For this purpose we used the *b*-value of $b = 0.94 \pm 0.05$ of the first part of the sequence before the Christchurch event to find the largest inferred aftershock m^* that was consistent with the data. The intersection of the fit line and the line $N = 1$ gave us a value of $m^* = 6.3$ and, therefore, $\Delta m^* = 0.8$ (see Fig. 2A). By using the data from the initial part of the sequence it was possible to estimate approximately the expected magnitude of the largest aftershock which occurred later in the sequence. Similar analysis was performed for the aftershock sequences of the two largest events with results shown in Figs. 2B and 2C. Although not considered in this analysis, a m_L 5.8 aftershock on 23 December 2011 was consistent with the post-June m^* estimate (Fig. 2C); this was followed 80 minutes later by a m_L 6.0 earthquake.

Aftershock decay rates

To model the decay of aftershock rates we can employ the modified Omori law (Utsu et al. 1995; Shcherbakov et al. 2004) to:

$$r(\geq m_c, t) \equiv \frac{dN}{dt} = \frac{1}{\tau(1 + t/c)^p}, \tag{3}$$

where t is time elapsed since the mainshock, m_c is a lower magnitude cut-off above which earthquakes are taken into account, τ and c are characteristic times and p is an exponent specifying how fast the sequence is decaying in time. Both τ and c may be considered functions of the lower magnitude cut-off m_c, and thus may be written as $\tau(m_c)$ and $c(m_c)$ (Shcherbakov et al. 2004).

To analyse the decay rates after the Darfield mainshock, we considered the same three time intervals used in the analysis of the frequency-magnitude statistics. All aftershocks above magnitude $m \geq 3.0$ were considered except for the 13 June 2011 event, where the lower cut-off was $m \geq 3.2$. The results are shown in Fig. 3 for the Darfield sequence during the first 171 days, for the Christchurch sequence for 112 days and for the 13 June 2011 earthquake sequence using 180 days. The constructed aftershock rates were modeled using the modified Omori law. The parameters of the model were computed using the maximum likelihood estimate (Utsu et al. 1995; Guo & Ogata 1997). The obtained values of the parameters are listed in Table 1. The corresponding fits are shown in Figs. 3A–3C as solid curves.

The Canterbury aftershock sequence can be also modelled by the combination of the three rates reflecting the occurrence of two large earthquakes which generated their own aftershock sequences:

$$r(\geq m_c, t) = \frac{1}{\tau_1\left(1+\frac{t}{c_1}\right)^{p_1}} + \frac{H(t-t_2)}{\tau_2\left(1+\frac{t-t_2}{c_2}\right)^{p_2}} + \frac{H(t-t_3)}{\tau_3\left(1+\frac{t-t_3}{c_3}\right)^{p_3}}. \quad (4)$$

Here $H(t-t_i)$ is a Heaviside step function and $t_2 = 171.3$ days and $t_3 = 282.4$ days are the times of occurrence of the Christchurch and the 13 June 2011 earthquakes since the

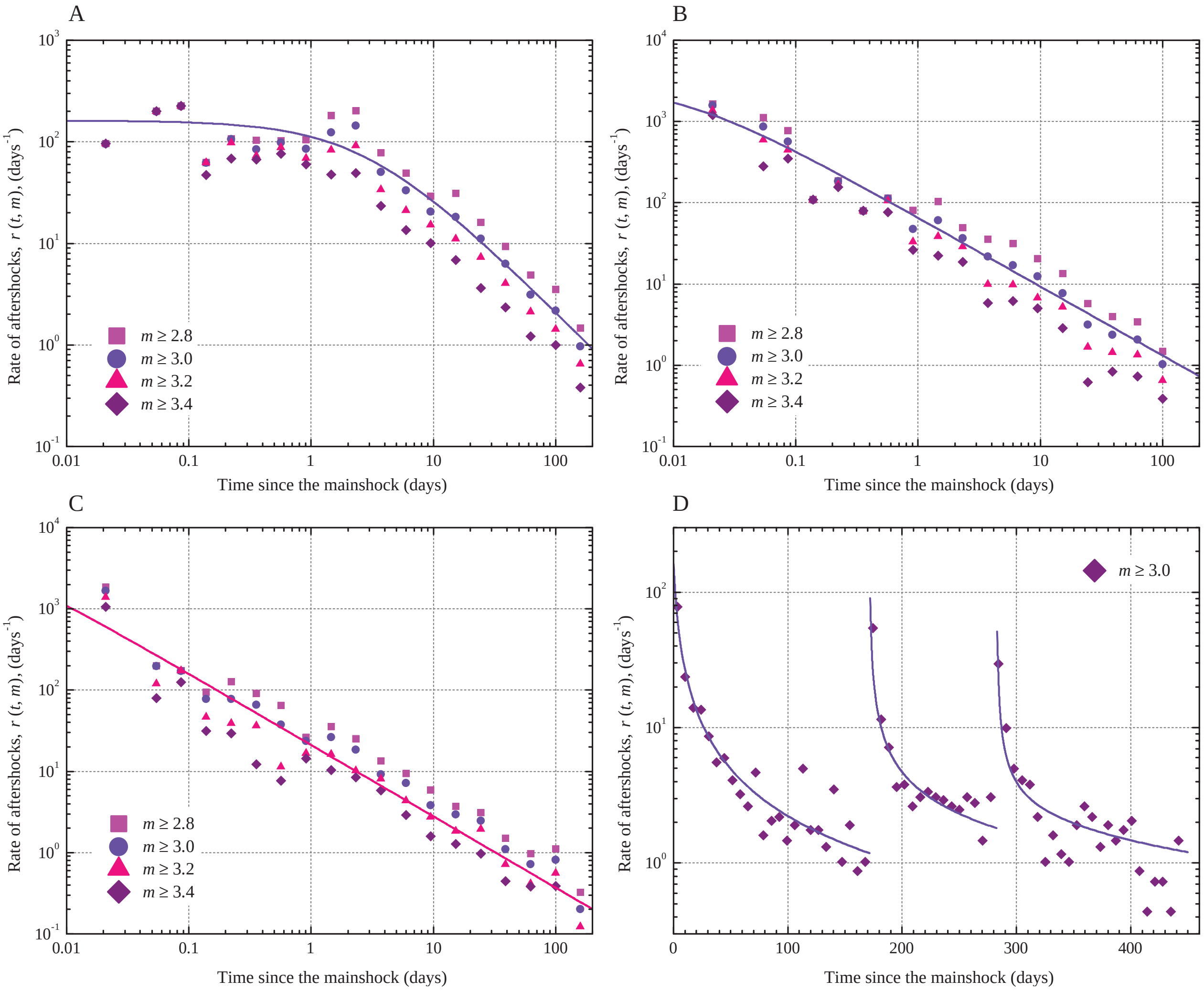

Figure 3 The rates of the occurrence of aftershocks are shown. **A,** For 171 days after the Darfield mainshock. **B,** For 112 days after the first Christchurch earthquake. **C,** For 180 days after the second Christchurch earthquake. **D,** For the entire Canterbury aftershock sequence. Lower magnitude cut-offs are taken to be $m \geq 2.8$ (squares), $m \geq 3.8$ (circles), $m \geq 3.2$ (triangles) and $m \geq 3.4$ (diamonds). The values of c, τ and p were calculated by fitting the data for all aftershocks with magnitudes greater than $m \geq 3.0$ given in A and B and above 3.2 in C to the modified Omori law, Equation (3), by the maximum likelihood method. To model the rates shown in D we used the compound rate given by Equation (4) for all events above magnitude 3.0.

Table 2 The parameter of the modified Omori law *c* estimated for the different magnitude cut-offs m_c. The last two rows show the parameters of the compound rate given by Equation (4) and computed for the whole sequence for all events above magnitude 3.0.

	Darfield mainshock	Christchurch event	13 June 2011 event
$c(m_c = 2.8)$	3.47 ± 1.30	0.016 ± 0.012	0.0020 ± 0.0026
$c(m_c = 3.0)$	2.80 ± 1.10	0.012 ± 0.010	0.0018 ± 0.0023
$c(m_c = 3.2)$	2.01 ± 0.94	0.010 ± 0.010	0.0012 ± 0.0019
$p_i(m_c = 3.0)$	1.20	0.86	0.90
$c_i(m_c = 3.0)$	2.88	0.013	0.0029

mainshock. The parameters of this model can be estimated by the maximum likelihood method; they are reported in Table 2 and the plot of the model is given in Fig. 3D.

To analyse the dependence of the rates on the lower magnitude cut-off thresholds, we also plotted the rates above several different cut-offs: $m \geq 2.8$, $m \geq 3.0$, $m \geq 3.2$ and $m \geq 3.4$. For all three sequences, the cut-off of $m \geq 2.8$ shows that the catalogue is not complete for the earlier times after the mainshocks. This is related to the early aftershock deficiency effect seen in the Parkfield aftershock sequence (Peng et al. 2006) and in Japan (Peng et al. 2007), where the number of aftershocks seen immediately after the mainshock is smaller than expected from the modified Omori law decay rate for the whole sequence even after correcting for completeness. Figure 3 shows that $c(m_c)$ systematically increases with decreasing m_c. This shows that the $c(m_c)$ value is more than merely an artefact of incompleteness in the early part of the catalogue as observed for other aftershock sequences around the world (Shcherbakov et al. 2004, 2005, 2006; Nanjo et al. 2007).

Conclusion

In this study, the scaling properties of the aftershock sequence of the M_W 7.1 (m_L 7.1) 2010 Darfield (Canterbury, New Zealand) mainshock were analysed. The sequence produced a reach behaviour by triggering two strong earthquakes of magnitudes m_L 6.3 (M_W 6.2) and m_L 6.4 (M_W 6.0) following the mainshock. Aftershocks of m_L 5.8 and 6.0 occurred on 23 December 2011, but were not considered in this study. In this respect, this sequence can be compared to the Landers earthquake, California, sequence where three large earthquakes produced their own rich aftershock sequences with the mainshock being preceded by a large foreshock (Joshua Tree event) and being followed by the large aftershock (Big Bear event).

The difference in magnitude (m_L) between the second-largest aftershock (Christchurch event) and mainshock is estimated to be ≈ 0.8 and comparable to the value Δm^* of ≈ 0.8 derived using the extrapolation of the GR scaling relation. It is important to note that the application of the modified Båth law in finding the inferred largest aftershock was successful in estimating the magnitude of one of the largest aftershocks which occurred later in the sequence.

The rates of decay of aftershocks were found to follow the modified Omori law for the three sequences considered. The $c(m_c)$ value was seen to be dependent on the lower magnitude cut-off m_c, with $c(m_c)$ decreasing as m_c increases. It was also shown that the sequence can be successfully modelled by a compound rate, including the secondary aftershocks generated by the two large earthquakes.

Acknowledgements

This work has been supported by NSERC Discovery grant 355632-2008 and UWO ADF grant R4203A03. We acknowledge the New Zealand GeoNet project and its sponsors EQC, GNS Science and LINZ for providing data used in this study. We also would like to thank Martha Savage and the other anonymous reviewer for their constructive criticism and comments which helped to improve the paper.

References

Båth M 1965. Lateral inhomogeneities of the upper mantle. Tectonophysics 2: 483–514.

Beavan J, Samsonov S, Motagh M, Wallace L, Ellis S, Palmer N 2010. The *M*w 7.1 Darfield (Canterbury) earthquake: geodetic observations and preliminary source model. Bulletin of the New Zealand Society for Earthquake Engineering 43: 228–235.

Beavan J, Motagh M, Fielding E, Donnelly N, Collett D 2012. Fault slip models of the 2010–2011 Canterbury, New Zealand, earthquakes from geodetic data, and observations of post-seismic ground deformation. New Zealand Journal of Geology and Geophysics, 55. doi: 10.1080/00288306.2012.697472

Ben-Zion Y 2008. Collective behavior of earthquakes and faults: Continuum-discrete transitions, progressive evolutionary changes, and different dynamic regimes. Reviews of Geophysics 46: RG4006. doi:10.1029/2008rg000260

Bender B 1983. Maximum-likelihood estimation of b-values for magnitude grouped data. Bulletin of the Seismological Society of America 73: 831–851.

Bhattacharya P, Phan M, Shcherbakov R 2011. Statistical Analysis of the 2002 *M*w 7.9 Denali Earthquake Aftershock Sequence. Bulletin of the Seismological Society of America 101: 2662–2674.

Console R, Lombardi AM, Murru M, Rhoades D 2003. Bath's law and the selfsimilarity of earthquakes. Journal of Geophysical Research 108: 2128. doi:10.1029/2001JB001651

Fry B, Benites R, Reyners M, Holden C, Kaiser A, Bannister S, Gerstenberger M, Williams C, Ristau J, Beavan J 2011. Strong shaking in recent New Zealand earthquakes. EOS 92: 349–351.

Guo ZQ, Ogata Y 1997. Statistical relations between the parameters of after- shocks in time, space, and magnitude. Journal of Geophysical Research 102: 2857–2873.

Gutenberg B, Richter CF 1954. Seismicity of the Earth and Associated Phenomenon, second edition. Princeton University Press, Princeton.

Guttorp P, Hopkins D 1986. On estimating varying b-values. Bulletin of the Seismological Society of America 76: 889–895.

Helmstetter A, Sornette D 2003. Bath's law derived from the Gutenberg-Richter law and from aftershock properties.

Geophysical Research Letters 30: 2069. doi: 10.1029/2003GL018186

Kisslinger C 1996. Aftershocks and fault-zone properties. Advances in Geophysics. 38, Academic Press, San Diego, 1–36.

Nanjo KZ, Enescu B, Shcherbakov R, Turcotte DL, Iwata T, Ogata Y 2007. Decay of aftershock activity for Japanese earthquakes. Journal of Geophysical Research 112: B08309. doi: 10.1029/2006JB004754

Peng ZG, Vidale JE, Houston H 2006. Anomalous early aftershock decay rate of the 2004 *M*w 6.0 Parkfield, California, earthquake. Geophysical Research Letters 33: L17307. doi: 10.1029/2006GL026744

Peng ZG, Vidale JE, Ishii M, Helmstetter A 2007. Seismicity rate immediately before and after main shock rupture from high-frequency waveforms in Japan. Journal of Geophysical Research 112: B03306. doi: 10.1029/2006JB004386

Quigley M, Villamor P, Furlong K, Beavan J, Van Dissen R, Litchfield N, Stahl T, Duffy B, Bilderback E, Noble D, Barrell D, Jongens R, Cox S 2010. Previously unknown fault shakes New Zealand's South Island. EOS, American Geophysical Union 91(49): 469–471.

Quigley M, Van Dissen R, Litchfield N, Villamor P, Duffy B, Barrell D, Furlong K, Stahl T, Bilderback E, Noble D 2012. Surface rupture during the 2010 *M*w 7.1 Darfield (Canterbury, New Zealand) earthquake: implications for fault rupture dynamics and seismic-hazard analysis. Geology 40: 55–58. doi:10.1130/G32528.1

Shcherbakov R, Turcotte DL 2004. A modified form of Bath's law. Bulletin of the Seismological Society of America 94: 1968–1975. doi: 10.1785/012003162

Shcherbakov R, Turcotte DL, Rundle JB 2004. A generalized Omori's law for earthquake aftershock decay. Geophysical Research Letters 31: L11613. doi: 10.1029/2004GL019808

Shcherbakov R, Turcotte DL, Rundle JB 2005. Aftershock statistics. Pure and Applied Geophysics 162: 1051–1076.

Shcherbakov R, Turcotte DL, Rundle JB 2006. Scaling properties of the Parkfield aftershock sequence. Bulletin of the Seismological Society of America 96: S376–384. doi: 10.1785/0120050815

Tinti S, Mulargia F 1987. Confidence intervals of b-values for grouped magnitudes. Bulletin of the Seismological Society of America 77: 2125–2134.

Utsu T, Ogata Y, Matsu'ura RS 1995. The centenary of the Omori formula for a decay law of aftershock activity. Journal of the Physics Earth 43: 1–33.

Vere-Jones D 1969. A note on the statistical interpretation of Bath's law. Bulletin of the Seismological Society of America 59: 1535–1541.